

## SCANNING OF FREE-FORM SURFACES BY USING A LASER-STRIPE SENSOR ON A CMM

*Fernández, P.<sup>1</sup>, Álvarez, B. J.<sup>1</sup>, Rico, J. C.<sup>1</sup>, Blanco, D.<sup>1</sup>, Valiño, G.*

<sup>1</sup> University of Oviedo, Gijón, Spain, jcarlosr@uniovi.es

**Abstract:** This research presents a working methodology for developing an automatic planning system of the scanning process of free-form surfaces. The surface has been modelled using a STL format, that permits the automatic recognizing of any type of surface. This work does only consider collision-free orientations that guarantee the visibility of the zone to scan and that are compatible with the constraints imposed by the process parameters. To speed up the calculation of these orientations, different methods like back-face culling and space partitioning techniques, such as kd-trees, are applied. Once the space occupied by the part is partitioned in regions, recursive ray traversal algorithms are used in order to check for intersection exclusively the part triangles (STL) that can potentially be traversed by each laser beam direction.

**Keywords:** scanning, laser, CMM

### 1. INTRODUCTION

In recent years, no contact scanning techniques based on laser systems have supposed an enormous progress [1]. Although it is not yet very extended, this technique provides a high speed for point acquisition that allows for obtaining thousands of points per second. The time reduction is extraordinary and consequently also the costs associated to the inspection process, mainly compared to other traditional contact-type methods.

Although it is true that some companies use this scanning technique already, the majority do it manually, being the operator who decides about the election of the process parameters and the working methodology to follow. Consequently, the scanning results have not the expected quality and it is difficult to reproduce identical process conditions, even when the scanned parts are identical or with similar characteristics. For this reason, there are a lot of research efforts made in order to analyse the influence of the parameters in laser scanning systems, such as the depth of view and the view angle [2] or in order to develop techniques for compensating the characteristic errors of this scanning technology [3]. Other research has mainly focused on the phase of reconstructing the scanned surfaces from clouds of points [3,4] and only few of them have approached the general problem of scanning process planning [5-7].

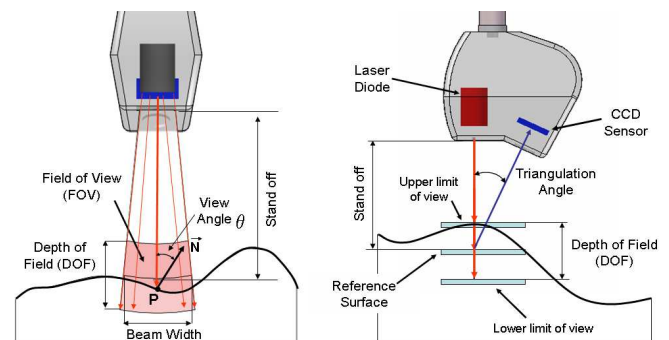


**Fig. 1. Parameters of the digitizing laser system**

The aim of this work is to develop a methodology for 3D scanning of free-form surfaces by using a CMM. This methodology has relation not only with the surface geometry or the scanning paths but also with the optimal orientation of the scanning sensor and the process parameters (laser intensity, depth of view, distance between laser stripe, etc.). With all this information, it will be possible to define the optimal working strategy for scanning a certain surface. As a consequence, higher quality results are achieved in lower process time

### 2. CHARACTERISTICS OF LASER SCANNING SYSTEMS

In laser scanning sensors a laser stripe of known width is projected onto a part surface and the reflected beam is detected by a CCD camera. By means of image processing based on a triangulation method, 3D coordinates of the surface points are acquired. Fig. 1 shows the main parameters of the laser system used in this work (LC-50 by Metris<sup>®</sup>).

Apart from these parameters, a laser scanning sensor like the one mentioned above fixes the distance between laser stripes, the distance between points within each stripe and the overlap zone between stripes.

To carry out the scanning process it is necessary a relative movement between the laser system and the surface. This movement consist not only on linear and/or angular displacements but also on orientation changes of the laser head or the surface. Hence, the laser system used in this work has been installed in the motorised head of a CMM (Global Image of Brown&Sharpe). This way, three possible

linear displacements (X, Y, Z) are available in combination with two rotations (A, B) of the machine head (PH10MQ). Since the head orientation changes are discrete (7.5°), 720 different orientations of the laser system can be achieved with regard to the scanning surface.



Fig. 2. Experiment for determining the limit view angle

### 3. CONSTRAINTS FOR POINT SCANNING

Some of the parameters shown in Fig. 1 are considered as constraints for scanning points on a surface. Some of them are imposed by the system manufacturer whereas other may be controlled by the user. Among the controlled parameters, the laser beam intensity and the laser head orientation stand out.

Influence of laser intensity in the scanning results has been analysed by means of several experiments. For instance, it has been proved that the laser intensity has to be adequate to the colour of the scanned surface. This way, dark coloured surfaces need higher intensity. Moreover, it has been demonstrated that the dispersion range of points over the theoretical surface increases with laser intensity.

In relation to the head orientation, this affects directly the *view angle*, which determines the zones of the scanned surface that can or not be acquired depending on its greater or smaller inclination. The number of points acquired has been considered as a criterion to determine if an orientation is better than any other. The experiment was based on digitizing the same planar surface varying the A angle of the laser head orientation. The higher number of points acquired has been reached for  $A=0^\circ$  and  $B=0^\circ$ , regardless the laser intensity used. That is, when the head is perpendicular to the surface. As the head direction changes with regard to the surface, it will be necessary a higher intensity to keep acquiring a high number of points. This way, an orientation (*limit view angle*) for which laser head does not acquire points can be found.

Another experiment has been carried out for determining the *limit view angle* (Fig. 2) by using a planar surface, in which its inclination has been increased until no points were acquired in the entire *field of view* (FOV). The limit view angle was found to be  $60^\circ$  for a white surface whereas this value can change for other colours. For instance, the limit view angle of a metallic surface will scarcely be  $15^\circ$  for an

optimal laser intensity and a perpendicular orientation of the head (without saturated points).

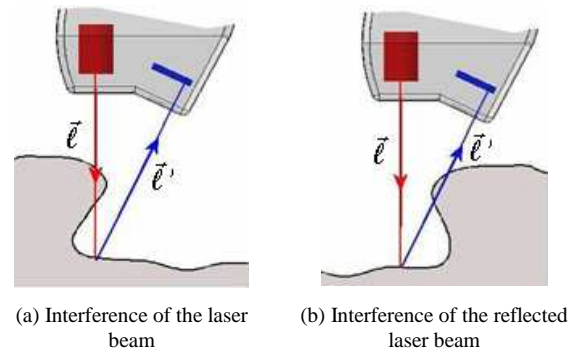


Fig. 3. Possible laser interferences with the surface

Besides, there are parameters that can not be controlled by the user and they are imposed by the equipment manufacturer, such as the *triangulation angle*. This angle is measured between the incident and the reflected laser beams. None of these laser beams must interfere with the part to make possible the acquisition of points (Fig. 3). For determining the *triangulation angle*, the device shown in Fig. 4 has been used. During the scanning of the lower surface (gauge block), an occlusion zone appears where the CCD sensor cannot acquire points because an interference between the reflected laser beam and the part occurs. The triangulation angle measured was found to be about  $25^\circ$ .

There exist several other influence factors such as roughness and reflectance of a surface and ambient illumination that have not been considered in this work.

### 4. SCANNING METHODOLOGY

The optimal beam orientation in laser scanning of a surface is perpendicular to this surface, as it occurs in contact inspection.

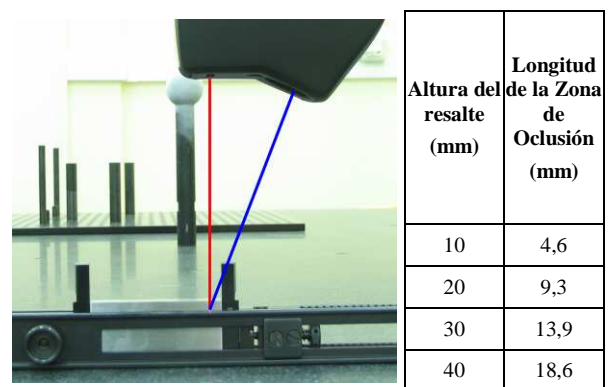


Fig. 4. Experiment for determining the size of the occlusion zone

Due to the shape of free-form surfaces, different points may be associated to different normal directions. In order to evaluate these directions a previous surface discretization has been carried out by means of the STL model. This format represents the surface by a set of planar triangles whose vertices and unit normal vectors are known. This simplification of the surface is suitable for scanning tasks

and it is less computing time consuming. This way, each triangle can be considered associated to a significant point of the surface and the unit normal vector of the surface (triangle) at this point can be obtained.

Since the optimal orientation of the laser head is perpendicular to the scanned surface, the proposed methodology deals with determining the optimal laser head orientations that are closest to the normal direction of each triangle (unit normal vector  $\vec{n}$ ). However, there can exist laser head orientations, non-optimal, that also allow for scanning the surface correctly. In both cases, for a head orientation  $\vec{l}$  to be considered as valid, the constraint imposed by the *limit view angle* must be taken into account. The measured limit view angle was found to be about  $60^\circ$ . In general, a space called *local cone* that includes the valid laser head orientations for each triangle of the discretized surface can be defined. The directions of the *local cone* must satisfy the next condition:

$$\cos 60^\circ < \vec{l} \cdot \vec{n} \leq 1 \quad (1)$$

Even so, these orientations  $\vec{l}$  of the local cone of each triangle may interfere with other triangles of the discretized surface (Fig. 3a). Therefore, for determining if an orientation  $\vec{l}$  is valid, the next condition must be checked:

$$\vec{l} \cap F_i = \emptyset \quad (2)$$

where  $F_i$  is any triangle of the discretized surface. Moreover possible occlusion zones due to interference between the reflected laser beam  $\vec{l}'$  and the part must be checked (Fig. 3b). To carry out this verification, the *triangulation angle* ( $25^\circ$ ) obtained in the experiment of the previous section has been used. Similarly to the direction  $\vec{l}$ , a direction  $\vec{l}'$  of the reflected laser beam will be valid if the next condition is satisfied:

$$\vec{l}' \cap F_i = \emptyset \quad (3)$$

Orientations of the local cone that satisfy the conditions (2) and (3) will be within a more restricted space called the *global cone*. This analysis procedure must be repeated for each triangle of the STL.

The computation of GAC is complex and expensive from a computational point of view, because it involves the calculation of multiple intersections. In order to accelerate the computation, a *back-face culling* algorithm that reduces the number of triangles to study in the global accessibility analysis has also been implemented. Thus, from the initial triangularized model  $W$ , a subset  $W'$  is extracted that do not include those triangles whose visibility according to an analysed laser beam direction is completely blocked by other triangles. In practice, the identification of facets that will be within  $W'$  will be carried out verifying the angle between the facet normal and the laser beam orientation. If this angle is greater than  $\pi/2$ , it is necessary to determine if there is interference between facet and laser beam. Otherwise, the facet will be discarded for the global analysis of that laser beam orientation.

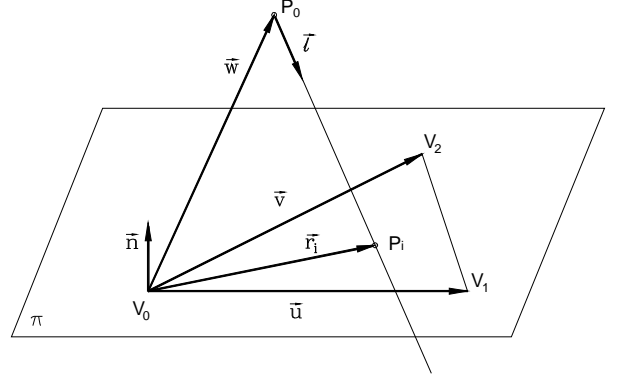


Fig. 5. Intersection between laser beam  $\vec{l}$  and a triangle facet  $V_0V_1V_2$

#### 4.1. Intersection between triangular facets and incident/reflected laser beam orientations

By using the STL format associated with the CAD model of the part, the facets will be triangles whose vertices  $V_0$ ,  $V_1$  y  $V_2$  and unit normal vector  $\vec{n}$  are known. Firstly, the implemented algorithm determines if there exist intersection between each incident laser beam orientation  $\vec{l}$  and all the triangles that constitute the part boundary. If the next equation (Fig.5) is satisfied:

$$\vec{n} \cdot \vec{l} = 0 \quad (4)$$

the orientation will be parallel to the supporting plane of the triangle and therefore there will be no intersection. If both the expression (4) and the next condition are satisfied:

$$\vec{n} \cdot \vec{w} = 0 \quad (5)$$

then the laser beam orientation will be contained in the plane and there will not be intersection either.

If none of the previous relations is fulfilled, then there is intersection between the incident laser beam and the supporting plane of the triangle. The intersection point  $P_i$  can be expressed as:

$$P_i = P_0 - \frac{\vec{n} \cdot \vec{w}}{\vec{n} \cdot \vec{l}} \cdot \vec{l} \quad (6)$$

Finally, it is necessary to check if this point  $P_i$  lies within the triangle defined by the three vertices  $V_0$ ,  $V_1$  and  $V_2$ . This verification is based on the algorithm developed by Möller and Trumbore [8]. From the equation of the supporting plane of the triangle  $V_0$ ,  $V_1$  and  $V_2$ :

$$V(s, t) = V_0 + s \cdot \vec{u} + t \cdot \vec{v} \quad (7)$$

a point  $P_i$  located on that plane will be within the triangle if there exist values  $s_i$  and  $t_i$  that satisfies the next equation:

$$P_i - V_0 = s_i \cdot \vec{u} + t_i \cdot \vec{v} \quad (8)$$

where  $s_i \geq 0$ ,  $t_i \geq 0$  and  $s_i + t_i \leq 1$ .

The values of the parameters  $s_i$  and  $t_i$  can be determined from the following expressions:

$$s_i = \frac{(\vec{u} \cdot \vec{v}) \cdot (\vec{r}_i \cdot \vec{v}) - (\vec{v} \cdot \vec{v}) \cdot (\vec{r}_i \cdot \vec{u})}{(\vec{u} \cdot \vec{v})^2 - (\vec{u} \cdot \vec{u})(\vec{v} \cdot \vec{v})} \quad (9)$$

$$t_i = \frac{(\vec{u} \cdot \vec{v}) \cdot (\vec{r}_i \cdot \vec{u}) - (\vec{u} \cdot \vec{u}) \cdot (\vec{r}_i \cdot \vec{v})}{(\vec{u} \cdot \vec{v})^2 - (\vec{u} \cdot \vec{u})(\vec{v} \cdot \vec{v})} \quad (10)$$

If the point lies within the triangle then there will be intersection and the analysis will continue with another triangular facet. Otherwise, a similar verification must be done for the reflected laser beam orientation. If there is still no interference, the laser beam orientation (incident and reflected) will be considered as valid.

#### 4.2. Intersections based on kd-trees

The use of space partitioning structures like kd-trees allows for reducing the number of intersection tests. It implies the intersection testing exclusively with facets that can potentially be traversed by each laser beam orientation (incident and reflected). The part is partitioned in regions bounded by planes and each part facet is assigned to the region within which it is located. Then, regions traversed by each laser beam orientation are selected and only intersections between this orientation and the facets included in these regions are tested.

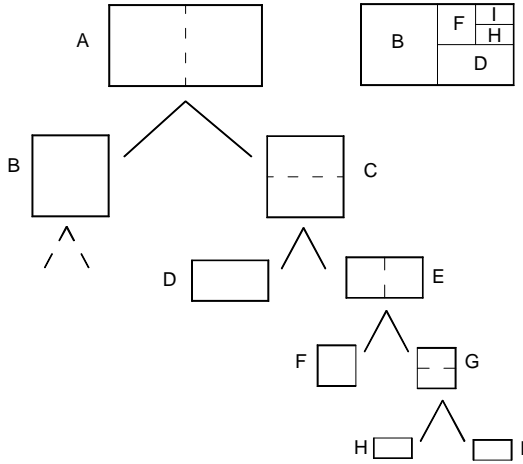


Fig. 6. Kd-tree representation of the space partitioning

This type of algorithms are similar to those of *binary space-partitioning* (BSP) tree type developed by Fuchs, Kedem and Naylor for calculating the visibility of a group of objects from an arbitrary point of view [9].

In the kd-tree case, the division of part in regions (*bounding boxes*) is carried out by means of axis-aligned splitting planes. This way, equations of these planes are simplified and consequently, the calculations of possible intersections. For determining the position of the splitting planes, the criterion chosen was to divide successively each region in two regions of the same size. Regards to the splitting sequence, the axis-aligned plane that is normal to the greater dimension of the region is always chosen in first place.

The partition of the part into successive regions can be represented by a binary tree whose root node stands for the

region that encloses the part completely (Fig. 6). Internal tree nodes are regions obtained in further partitions and leaf nodes represent regions into which the part is finally divided. Along with the associated region, each node of the tree stores information about the facets included, the plane that will be used for its further partitioning, and references to its children. The number of part subdivisions is equivalent to the number of levels or depth of the tree.

#### 4.3. Kd-tree traversal

Once kd-tree has been built it is necessary to apply an algorithm for identifying the sequence of leaf nodes that are intersected by each laser beam orientation. This algorithm is called *ray traversal algorithm* and was first developed and applied to a BSP tree by Kaplan [10].

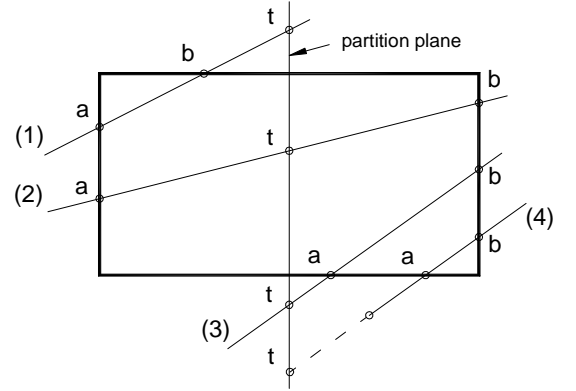


Fig. 7. Possible intersection cases between the laser beam and the regions determined by a splitting plane

The algorithm chosen in this paper corresponds to a variant of the algorithm developed by Kaplan. In particular, an algorithm of recursive type (*recursive ray traversal algorithm*) has been applied. When a ray (laser beam orientation) enters an interior node (region) of the kd-tree, which has two child nodes, the traversal algorithm decides if both of them are to be traversed by the ray and in which order. According to the position of the origin of the ray with regard to the splitting plane, the algorithm classifies the child nodes of the current interior node of the tree as “near” node and “far” child nodes. When the ray traverses only the “near” child node, then the algorithm descends to this node and recurses applying itself to this new node. When the ray has to visit both child nodes, then the algorithm saves the information about the “far” child node and descends to the “near” child node to repeat the checking process. When no facet is found to be intersected inside the “near” child node, the “far” child node is retrieved and the algorithm starts at that “far” child node again.

In order to determine if the ray only traverses the near child node or both child nodes, the algorithm compares the signed distances from the origin of the ray to the splitting plane ( $t$ ) and to the entry ( $a$ ) and exit ( $b$ ) point of the ray with regard to the node (Fig. 7).

When the traversal of the tree reaches a leaf node, the laser beam orientation is checked for intersection with the facets inside that node. If intersection exists, this orientation is considered not valid. Otherwise, it will be necessary to

analyse the intersection of the orientation with the rest of the nodes that it traverses. A laser beam orientation (incident and reflected) will be valid if there is no intersection with any facet contained in the nodes that it traverses.

Then, in order to reduce the number of sensor orientations it will be necessary to check if there exist at least one direction that allows for a complete scanning of the surface. This way, one or more laser head orientations common to all global cones must be looked up. Among these orientations, any of them can be chosen to scan the whole surface. Generally, the orientation to choose will be the optimal one or the closest to the optimal. Otherwise, if no orientations are found, the scanning of the surface will be done combining several laser head orientations.

## 5. RESULTS

The developed system determines the zones of the surface that can be scanned with different laser head orientations. For instance, Fig. 8 shows, by means of a grey scale, the triangles or zones of the surface whose normal directions coincide (darker colour) or separate (lighter colour) from different laser head orientations. This way, normal directions of the black coloured triangles are coincident with the proposed orientation (A, B) of the head. They are optimal orientations. The rest of triangles can be scanned with this orientation but the scanning quality gets worse as the head orientation separates from the normal of each triangle (grey coloured). White coloured triangles cannot be scanned by the selected head orientations (occlusion zones).

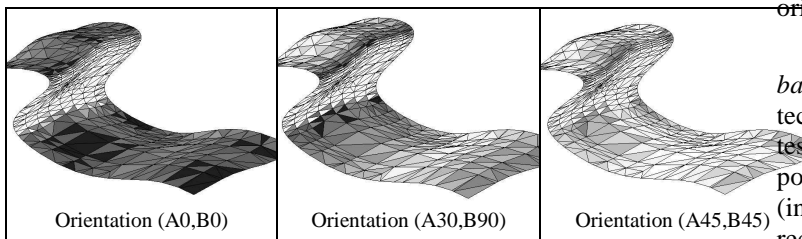


Fig. 8. Surface triangles that can be scanned with different laser head orientations

For the same example part (Part 1) the local and global cones for any triangle of the surface have been obtained. Fig. 9 shows the head orientation map associated to the local and global cones of two different triangles of the part surface. To simplify the visualization of the orientation map, increments of  $15^\circ$  have been considered for angles A and B.

As can be seen, triangles 284 and 708 present wide local orientation maps (local cone) that are very similar, where A is exclusively limited by the limit view angle ( $60^\circ$ ) and where B varies from  $0^\circ$  to  $360^\circ$  for almost every value of A. This is because the possible interference between the head orientation and the surface triangles are not considered for determining the local cones. The main difference between the two maps is the optimal orientation, which depends on the normal direction of each triangle. So, for triangle 284, the optimal orientation corresponds to  $A=15^\circ$  and  $B=75^\circ$  or

$90^\circ$  while for triangle 708 it corresponds to  $A=15^\circ$  and  $B=210^\circ-255^\circ$ .

Different are also the orientation maps corresponding to the global cones of each triangle. In this case it is relevant the location of the analysed triangle. For a triangle 708 which is away from possible occlusion zones there is no influence of potential obstacles over the incident and the reflected laser beam. For this reason the global and local cones are coincident. This not occurs for triangle 284, whose global cone is widely reduced with regard to the local one, due to its proximity to the occlusion zone of the surface. In these cases many of the incident and reflected laser beam orientations interfere with the surface and therefore they are eliminated. Even for triangle 284 the optimal orientations are eliminated when the global orientation map is constructed. Similar results have been obtained for the second part (Part 2) included in Fig. 9.

## 6. CONCLUSIONS

They have been made the first moves for developing a methodology which allows for an automatic scanning process planning applied to free-form surfaces.

Discretization of free-form surfaces by STL models allows for applying the developed method to scan any part, regardless of its constituent surfaces. By means of the STL format it is possible to know the normal direction for each triangle and therefore, the laser beam orientations that allow for visualizing and scanning it. The valid orientations of laser beam are constrained by the *limit view angle* and the *triangulation angle*. The former determines the local cone orientations and the latter the global cone.

To accelerate the calculation of possible intersections *back-face culling* algorithms and space partitioning techniques like kd-trees have been applied. It consists on testing for intersection exclusively the facets that can potentially be traversed by each laser beam orientation (incident and reflected). Once the kd-tree has been built, a recursive algorithm has been applied for identifying the sequence of leaf nodes that will be intersected by each laser beam orientation.

The method has been proved and applied to several free-form surfaces. This work includes the results obtained for two of these surfaces.

As future work the planning system will be completed by determining the group or groups of orientations common to the global cones associated to all triangles of the surface. These common orientations will be the minimum set of orientations needed for the complete scanning of the surface. Once this minimum set has been determined, the scanning trajectories can be established.

## ACKNOWLEDGEMENTS

This work is part of the results obtained in a research project supported by the Spanish Education and Science Ministry (MEC-04-DPI2004-03517) and FEDER.

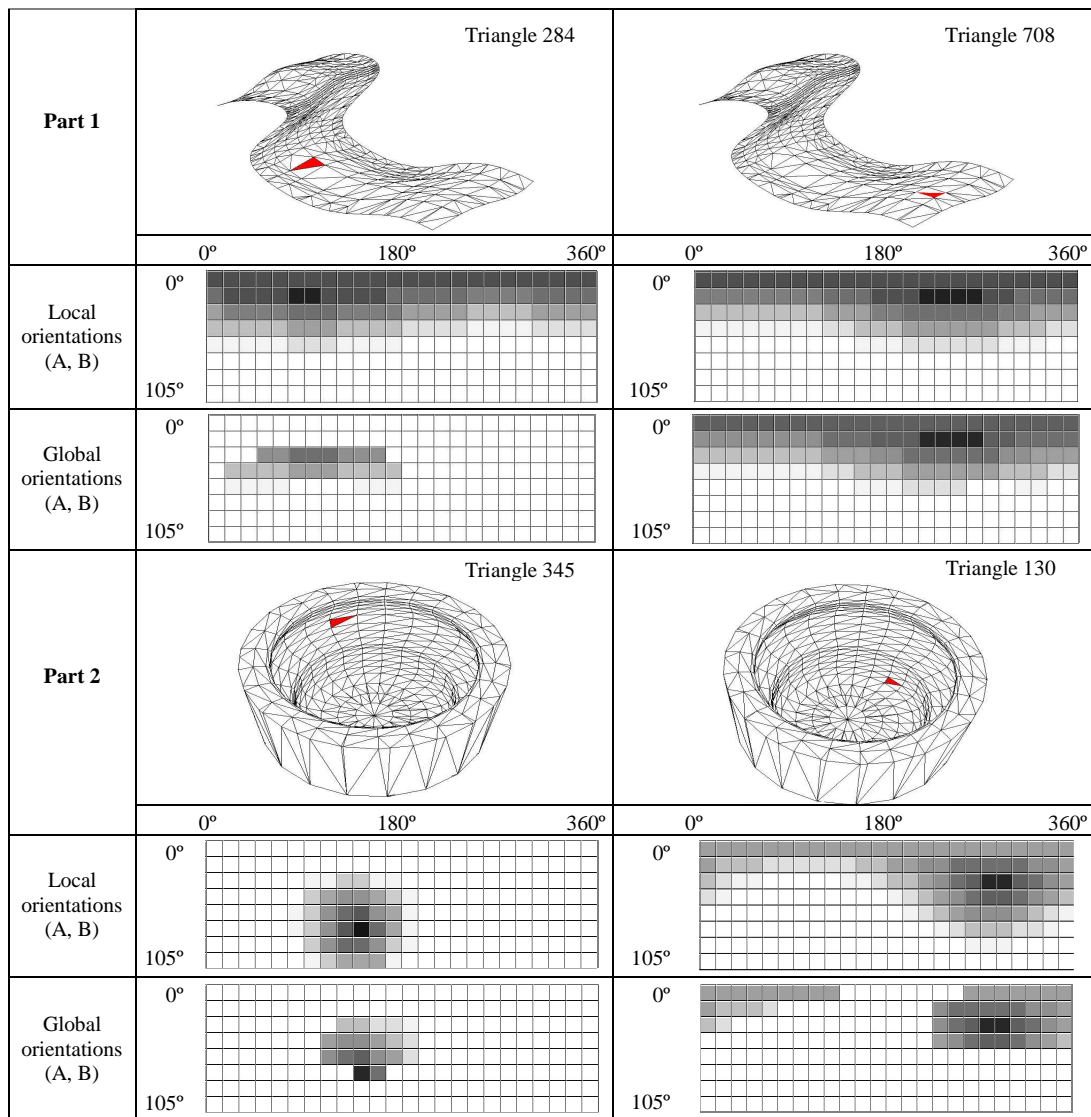


**Fig. 9. Orientation maps for two triangles of two example parts**

## REFERENCES

- [1] F. Blais, "A review of 20 years of range sensor development", Proceedings of the SPIE-IS&T Electronic Imaging, Vol. 5013 pp. 62-76, 2003.
- [2] H.-Y. Feng, Y. Liu and F. Xi, "Analysis of digitizing errors of a laser scanning system", Precision Engineering, Vol. 25, pp. 185-191, 2001.
- [3] L. Xinmin, L. Zhongqin, H. tian and Z. Ziping, "A study of a reverse engineering system based on vision sensor for free-form surfaces", Computers & Industrial Engineering, Vol. 40, pp. 215-227, 2001.
- [4] L. Li, N. Schemenauer, X. Peng, Y. Zeng and P. Gu, "A reverse engineering system for rapid manufacturing of complex objects", Robotics and Computer Integrated Manufacturing, Vol. 18, pp. 53-67, 2002.
- [5] Kwan H. Lee and Hyun-pung Park, "Automated inspection planning of free-form shape parts by laser scanning", Robotics and Computer Integrated Manufacturing Vol. 16, No. 4, pp. 201-210, 2000.
- [6] Seokbae Son, Hyun-pung Park and Kwan H. Lee, "Automated laser scanning system for reverse engineering and inspection", Int. J. of Machine Tools & Manufacture Vol. 42, No. 8, pp. 889-897, 2002.
- [7] F. Xi and C. Shu, "CAD-based path planning for 3-D line laser scanning", Computer-Aided Design Vol. 31, No. 7, pp. 473-479, 1999.
- [8] T. A. Möller and B. Trumbore, "Fast, minimum storage ray/triangle intersection", Journal of graphics tools, Vol. 2, pp. 21-28, 1997.
- [9] H. Fuchs, Z. M. Kedem and B. F. Naylor, "On visible surface generation by a priori tree structures", Proceedings of the SIGGRAPH-80, Vol. 14, pp. 124-133, 1980.
- [10] M. Kaplan, "Space-tracing: A constant time ray-tracer", Proceedings of the SIGGRAPH-85, Vol. 19, pp. 149-158, 1985.